

Electronic structure of red mercuric iodide

D. E. Turner and B. N. Harmon

*Microelectronics Research Center, Institute of Physical Research and Technology,
and Department of Physics, Iowa State University, Ames, Iowa 50011*

(Received 17 February 1989)

The self-consistent, relativistic electronic structure of tetragonal mercuric iodide has been calculated. Significant differences are found with the previously reported band structure (e.g., a direct rather than indirect gap is obtained). The conduction band is nearly isotropic for this layered crystal structure, while the iodide p -like valence band is quite anisotropic. The charge transfer between muffin-tin spheres centered on Hg and I sites is small, indicating very little ionic bonding, while the band structure provides clear evidence of strong covalent bonding.

I. INTRODUCTION

Mercuric iodide is a tetragonal, red semiconductor with a measured band gap of 2.13 eV at 20°C, corresponding to absorption for wavelengths of 585 nm and shorter.¹ At 127°C, there is a transformation to an orthorhombic structure (yellow phase) which persists up to the melting point of 259°C. While earlier studies were concerned with the optical properties and particularly the study of the excitonic spectrum, more recent work has focused on the transport properties and has been motivated by the possible use of HgI₂ in γ -ray spectrometers. Such applications have been hindered by the rather small hole mobility (~ 4 cm²/Vs at room temperature along the c axis²). Recent measurements on HgI₂ single crystals grown on board the space shuttle have suggested a somewhat larger value for the hole mobility,³ which raises questions concerning the intrinsic value for the hole mobility at room temperature, and what role impurities or defects may play. As a first step toward answering these questions, we have performed a modern first-principles calculation to determine the band structure and effective masses. We find significant differences with a previous band-structure calculation which was nonrelativistic and non-self-consistent.⁴

The space group for HgI₂ is D_{4h}^{15} . The primitive tetragonal unit cell with two formula units is shown in Fig. 1. Each mercury atom is tetrahedrally coordinated with four iodine atoms as illustrated in Fig. 2. The nearest-neighbor Hg-I spacing is ~ 2.78 Å. The nearly cubic close-packed arrangement for the iodine-iodine coordinations are 4I-I at 4.14 Å, 4I-I at 4.36 Å, and 4I-I at 4.64 Å. The tetragonal lattice constants are $a=b=4.361$ Å and $c=12.450$ Å at room temperature.⁵ The Hg-Hg distance in the ab plane is 4.361 Å and the Hg-Hg distance between planes is 6.95 Å. There are two layers of iodine atoms between each pair of Hg planes. Viewed in this layered fashion, one might expect HgI₂ to have rather anisotropic properties. However, the measured electron mobilities parallel and perpendicular to the c axis are comparable.² We will discuss this further after we present the results of the electronic structure.

II. CALCULATIONAL DETAILS

HgI₂ is one of several semiconductors considered for use in γ -ray spectrometers. Because of the strong dependence of the cross section on atomic number, high- Z materials are desirable for detectors. For Z above about 50, relativistic effects become very significant in determining electronic properties, and for elements as heavy as Hg a relativistic treatment of the electronic structure is essential. We have included relativistic effects in our calculations by first iterating to self-consistency using a scalar-relativistic method in which spin-orbit coupling is dropped, but all other relativistic contributions are included.⁶ The spin-orbit interactions were then added perturbatively for the final iteration. The local-density approximation of Hedin and Lundqvist was used for exchange and correlation.⁷ Eight k points on a uniform mesh in the irreducible $\frac{1}{16}$ of the Brillouin zone were used to calculate the wave functions and charge densities for each iteration. Iterations were continued until the difference between input and output charge in any muffin-tin (MT) sphere was less than $0.003e$. For the final three iterations, the mesh of k points was increased to 24. The scalar-relativistic calculations were performed using an efficient version of the Korringa-Kohn-Rostoker (KKR) method, while the spin-orbit coupling and final determination of the band structure along all of the symmetry lines were performed with the linear augmented-plane-wave (LAPW) method.⁸ The switching from the KKR to the LAPW method was strictly a matter of convenience in working with our present set of codes, since given the same potential the two methods yield essentially identical results. For these and similar methods, the unit-cell volume is partitioned with nearly touching spheres surrounding the atomic positions. Since the accuracy of these methods is highest when the total volume inside these so-called muffin-tin spheres is greatest, we inserted three more types of interstitial spheres, bringing the total number of muffin-tin spheres to 16. The total volume inside all the spheres was then 60.65% of the total volume. Figure 3 shows how these extra interstitial spheres help to fill the space between the atomic spheres.

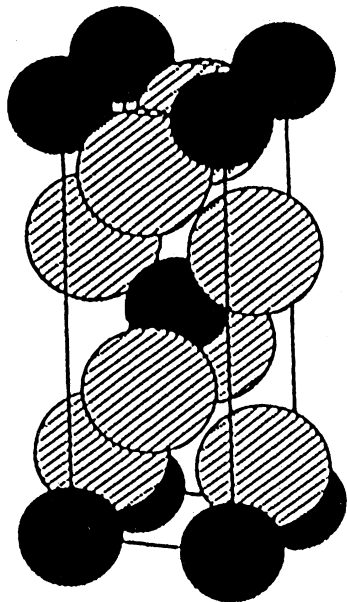


FIG. 1. The primitive tetragonal unit cell for HgI_2 . The mercury atoms are shown as solid and the iodine atoms are hatched.

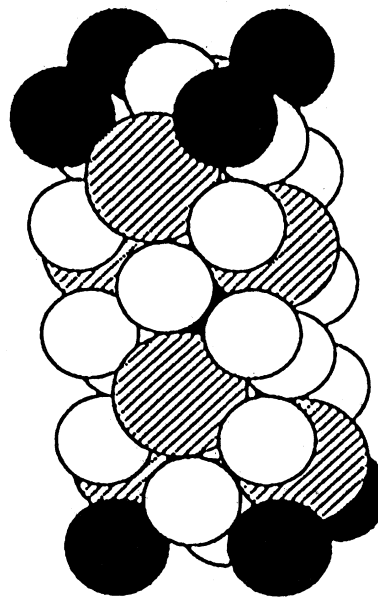


FIG. 3. The primitive unit cell of HgI_2 as in Fig. 1, but with the additional interstitial spheres shown open.

The position of the atoms and interstitial spheres, along with the sphere radii, are given in Table I.

III. RESULTS

A. Charge transfer

The initial starting potential was created by overlapping the self-consistent atomic charge densities with the $5d^{10}6s^2$ valence configuration for Hg and the $5s^25p^5$

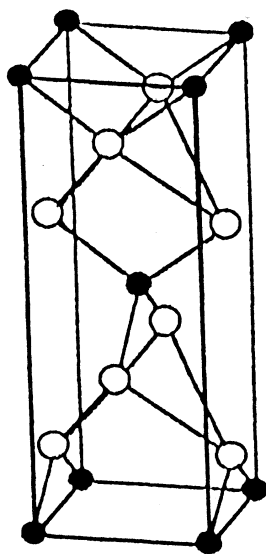


FIG. 2. The primitive HgI_2 unit cell drawn to emphasize the tetrahedral coordination of the mercury atoms.

configuration for I. Since the same exchange and correlation potential approximations were used for the atomic and solid calculations, the amount of charge transferred between Hg and I spheres gives some indication of the ionicity. In Table II, we list the charges inside each of the muffin-tin spheres for the overlapping neutral atoms (first iteration) and the final self-consistent iteration. It can be seen from Table II that there is a small charge transfer away from the Hg sphere and to the I sphere; however, the dominant effect is the transfer of charge out of the added muffin-tin spheres to both the I spheres and the interstitial region. Because such a large part of the valence charge is associated with either the added spheres or the interstitial region, it is not readily apparent how to assign a value to the ionicity. This is a common problem with methods which partition space and do not use an atomic wave function basis set for which the familiar treatments of ionicity are more meaningful. That is not to say the final charge density in the solid is inaccurate (*it is accurate*), but rather that the assignment of charge to different atoms is somewhat arbitrary with the present method. Nevertheless, the rather small charge transfer evident in Table II is indicative of much less ionicity than the $\text{Hg}^{2+}, \text{I}_2^-$ ionic assignment made by some authors. To confirm this point, we calculate the charge inside each muffin-tin sphere that results from overlapping the charge density of Hg^{2+} and I^- ions. The results are given in the last column of Table II. We see that the self-consistent charge inside the Hg sphere is much closer to the overlapping neutral-atom result, while the self-consistent charge inside the iodine sphere is about one-third of the way between the neutral-atom result and the ionic result. Clearly, such comparisons are suggestive, but cannot be used for precise quantitative analysis. Furthermore, we argue below that covalent bonding is

TABLE I. List of the atomic positions [relative to the lattice constants for the tetragonal unit cell ($a=b=4.37 \text{ \AA}$ and $c=12.44 \text{ \AA}$, see Ref. 1)] and the positions of the additional muffin-tin (MT) spheres which were included. The sphere radii are also given in atomic units (1 a.u. = 0.529172 \AA). The total volume inside the spheres is 972.343 a.u.^3 , or 60.65% of the unit-cell volume.

Type	Number	Position Vector			Sphere radius (a.u.)
		x	y	z	
Hg	1	0.0	0.0	0.0	2.555
	2	0.5	0.5	0.5	
I	1	0.0	0.5	0.139	2.636
	2	0.5	0.0	0.361	
	3	0.0	0.5	0.639	
	4	0.5	0.0	0.861	
MT 1	1	0.5	0.5	0.25	2.185
	2	0.5	0.5	0.75	
	3	0.0	0.0	0.25	
	4	0.0	0.0	0.75	
MT 2	1	0.5	0.0	0.111	2.326
	2	0.0	0.5	0.389	
	3	0.5	0.0	0.611	
	4	0.0	0.5	0.889	
MT 3	1	0.0	0.0	0.5	2.555
	2	0.5	0.5	0.0	

dominant and that if an assignment of ionicity is to be made, it should be less than $\text{Hg}^{+0.1}$.

B. Energy bands

The Brillouin zone for the tetragonal lattice is shown in Fig. 4. The calculated bands near the energy gap are shown in Fig. 5 along the high-symmetry lines. The four I $5s$ bands are positioned between -0.69 and -0.64 Ry and are not shown. Also not shown are ten Hg $5d$ bands centered near -0.25 Ry . The lowest two bands shown in Fig. 5 are between -0.10 and -0.03 Ry and can be described as Hg $6s$ and I $5p_z$ bonding bands. The next set of 10 bands between 0.025 and 0.26 Ry arise from the I $5p$ states. Without spin-orbit coupling, the top two bands in this group are degenerate at the Γ point and are composed of I p states with admixtures of the p_x and p_y orbitals. These bands at Γ are split by the spin-orbit interaction. The next two bands are the antibonding bands comprised of Hg $6s$ and I $5p_z$ states. These bands are just above the gap and are unoccupied.

TABLE II. The total electronic charge inside each of the muffin-tin (MT) spheres for the first iteration (overlapping neutral atoms), for the final self-consistent iteration, and for overlapping Hg^{2+} and I^- ions.

Sphere	Overlapping atoms	Self-consistent	Overlapping ions
Hg	78.595	78.555	77.928
I	50.965	51.032	51.090
MT 1	0.256	0.163	0.366
MT 2	0.207	0.202	0.200
MT 3	0.351	0.317	0.430
Interstitial	8.398	8.644	8.660

The calculated gap is direct and occurs at the zone center. The magnitude of the calculated gap is 0.52 eV , which is considerably less than the experimental value of 2.37 eV at 4.2 K .⁹ While some of this discrepancy may arise from our use of a muffin-tin potential rather than a general potential, we suspect that most of the difference is caused by the need to consider self-energy corrections for the excited states of the system. This is a common situation encountered when using the density-functional theory for semiconductors; and while known corrections can be applied to get a much better value for the band gap,¹⁰ the required calculations are difficult and would not change significantly the other aspects of the band structure of concern in this paper.

A previous band-structure calculation was performed using an empirical pseudopotential.⁴ In that calculation there was no self-consistency to allow for charge transfer and no relativistic effects included. The published bands from that calculation look much different than ours (partly because they were calculated using an incorrect body-centered-tetragonal unit cell), and we therefore will not make further reference to them.

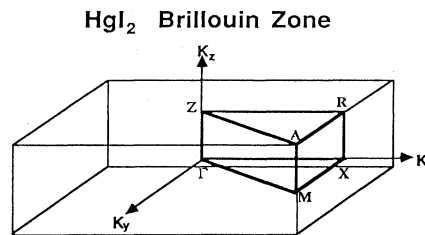


FIG. 4. The Brillouin zone for HgI_2 showing the irreducible $\frac{1}{16}$ section and high-symmetry points.

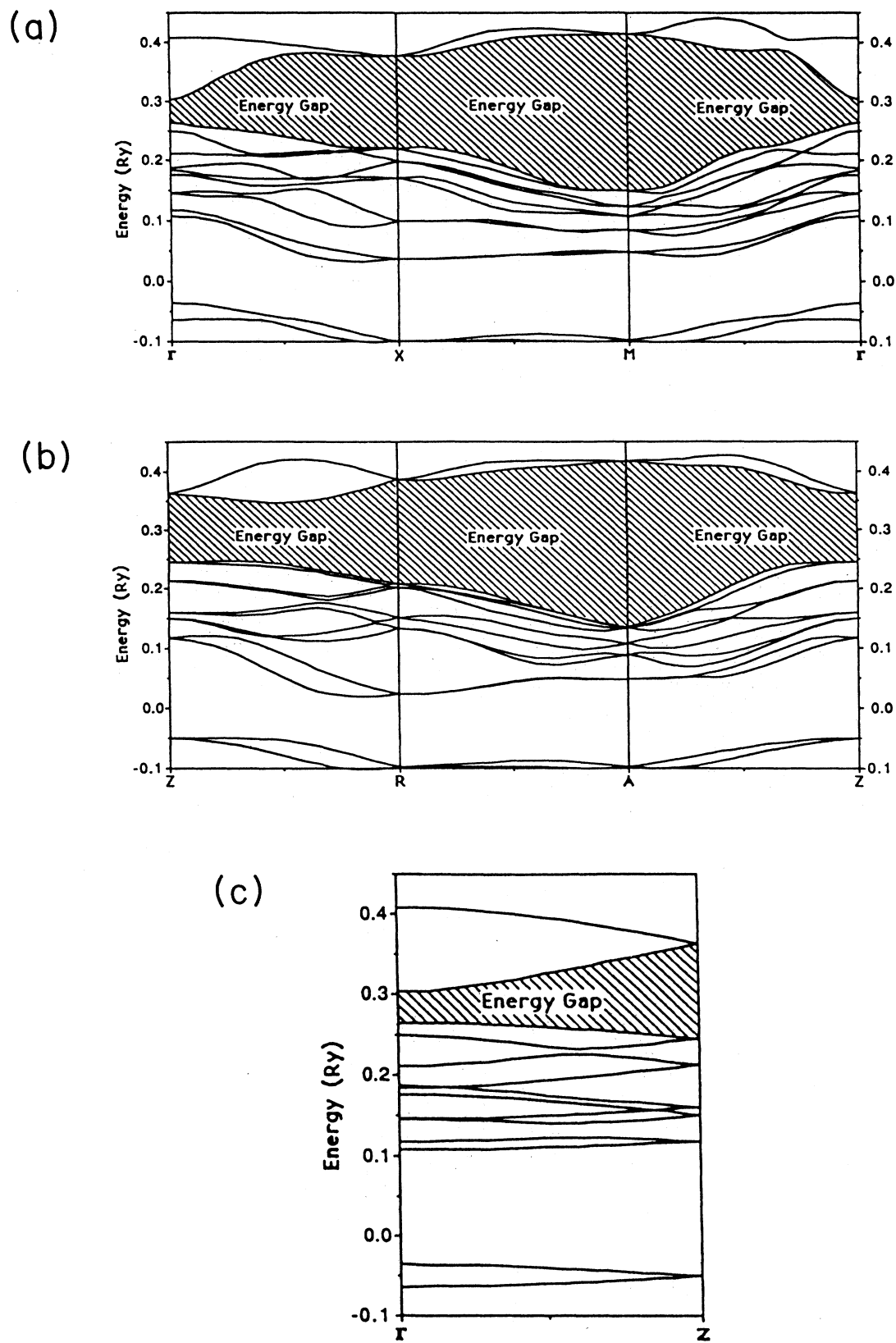


FIG. 5. (a) The energy bands of HgI_2 along the Γ -X-M- Γ symmetry directions. (b) The energy bands of HgI_2 along the Z-R-A-Z symmetry directions. (c) The energy bands of HgI_2 along Γ -Z.

C. Density of states

While we are unaware of any photoemission studies of HgI_2 , and do not expect any very soon because of this material's high vapor pressure, we have calculated the density of states for illustrative purposes. Each of the bands were fitted with a Fourier series consisting of 40 symmetrized plane waves (the average rms error was ≈ 1.5 mRy). These fits were then used along with the tetrahedron method¹¹ to generate the density-of-states curve shown in Fig. 6. A description of the bands to be found in each clearly split-off region of energy was given in the previous section. The mercury $5d$ bands are spin-orbit split by about 0.13 Ry, which is close to the atomic value. The $5d$ bands themselves are very narrow—indicative of their corelike nature. The Hg $6s$ and I $5p_z$ bonding and antibonding levels are split nearly evenly on both sides of the I $5p$ complex of bands. These split-off levels play a key role in the electronic structure of mercuric iodide, and confirmation of the bonding band level by photoemission or other experimental techniques would be welcome. Also shown in Fig. 6 is the density of states for the lowest two Hg $6p$ bands. These and higher bands arise from orbitals which are rather diffuse, and they begin to exhibit more free-electron-like behavior.

Figure 7 shows a blow up of the density of states for the valence and conduction bands near the gap. The rather low density of states at the bottom of the conduction band is just visible.

D. Effective masses

The effective masses for the top two valence bands and the conduction band were determined by fitting the calculated $E(\mathbf{k})$ near Γ with a polynomial. Table III summarizes the results of the analysis. These bands are nearly isotropic in the ab plane. The valence bands have much larger effective masses along the z axis, indicative

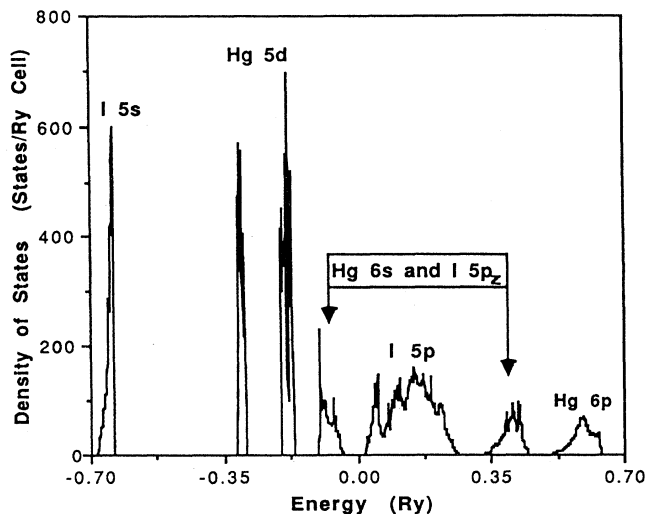


FIG. 6. The density of states for HgI_2 from -0.7 to $+0.7$ Ry.

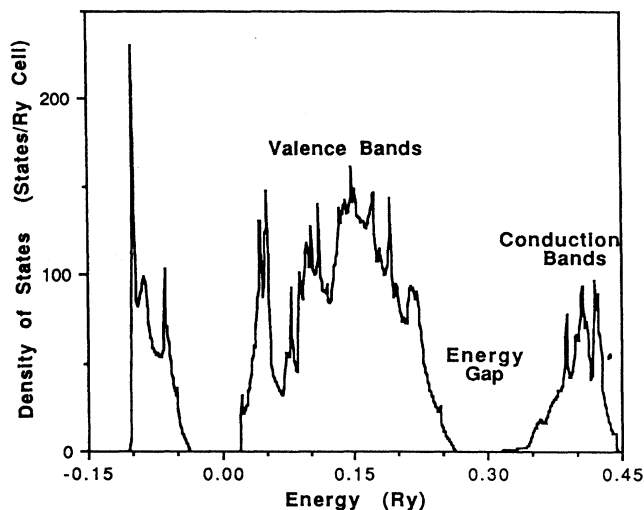


FIG. 7. The density of states for HgI_2 for the energy region near the gap.

of a layered material, while the conduction band exhibits considerably less anisotropy. A further discussion of the anisotropy in terms of the wave-function character is given in the next section.

IV. DISCUSSION

In this section, we first discuss the overall bonding and then describe in more detail the nature of the states near the gap. Finally, some observations about the mobility are made, although it is clear that a full knowledge of the phonon spectrum will be required to evaluate the intrinsic mobility.

A. Bonding

At first approach, one might think that HgI_2 would be composed of Hg^{2+} and I_2^- ions; however, this is far from the case. The ionization energy for the atomic Hg $6s$ valence electron is 10.437 eV and for the atomic I $5p$ electron 10.451 eV. In the solid, these states also have nearly the same energy and form bonding and antibonding bands with close to the same amount of Hg $6s$ and I $5p_z$ character in each set of bands. In the density of states, Figs. 6 and 7, it is clear that these bonding and antibonding states (two bands each) are split evenly on either side of the "nonbonding" I $5p$ states. Since the Hg $6s$ and I

TABLE III. The effective masses determined along the ΓX , ΓM , and ΓZ directions for the valence and conduction bands. The values are relative to the rest mass of the electron.

	Valence	Conduction
ΓX	0.167	0.106
ΓM	0.184	0.114
ΓZ	0.781	0.153

$5p_z$ bonding bands are occupied, and the antibonding are not, there is a strong net covalent bonding present. Our results for charge transfer suggest a small amount of ionicity, but probably no more than $\text{Hg}^{+0.1}\text{I}_2^{-0.05}$ would be appropriate for an ionic model. We arrived at this estimate by making atomic calculations. First, the neutral atoms gave essentially the same energy for both the Hg $6s$ level and the j weighted average level for the I $5p_{3/2}$ and $5p_{1/2}$ states. For both atoms, these energy levels shifted downward by approximately 0.06 Ry for every $0.1e$ removed from the valence shell. Since the bonding and antibonding bands are split *evenly* on each side of the I $5p$ levels, the ionicity must be small or an asymmetry would result. We might also point out that the crystal would quickly become unstable between the iodine-iodine layers if the iodine ions possessed a substantial net charge. Since these layers do separate easily, some ionicity is certainly present.

As mentioned earlier, when giving the effective masses, the conduction band is not particularly anisotropic. This is because the wave function for the conduction band at Γ is composed almost equally of Hg $6s$ and I $5p_z$ states, which maintain a strong coupling along the z axis. The valence band near Γ , on the other hand, is composed predominantly of I $5p_x$ and $5p_y$ states so that coupling along the z axis is weak and the effective mass large. Without spin-orbit coupling, there are four sets of degenerate I $5p_x$ and $5p_y$ bands at Γ . With spin-orbit coupling, each of these degenerate pairs would be split by approximately $\frac{2}{3}$ the atomic $5p_{3/2}$ - $5p_{1/2}$ splitting,¹² or about 0.7 eV; however, once the spin-orbit coupling is turned on, there is considerable mixing among these bands. The uppermost valence band has I $5p_{j=3/2}$ character with an antibonding phase among the I sites.

The nature of the bonding is reflected in the C_{66} elastic constant which is unusually small for HgI_2 .¹³ This is consistent with the directional nature of the Hg $6s$ -I $5p_z$ covalent bonds which do not provide any "cross-bracing" bonds to oppose shear within the ab plane.

B. Phonons and mobility

The relatively low hole mobility at room temperature was one of the motivations for undertaking the present study. While a full calculation of the mobility (due to phonon scattering) is well beyond the scope of this present study, there are a few points worth mentioning. To the extent that phonon scattering of electrons is isotropic (somewhat questionable for this material) our effective-mass results suggest that the hole mobility in the ab plane should be about 5 times larger than along the c axis.¹⁴ The electron mobility would only be 1.4 times greater in the ab plane.

An understanding of the room-temperature mobility will require further knowledge of the phonon spectrum than is presently available. With 6 atoms per unit cell, there are 18 phonon branches. Only the lower six branches have been measured by inelastic neutron scattering,¹⁵ and all the measured frequencies from these branches are below 1.2 THz ($h\nu/k \approx 58$ K). Infrared and Raman measurements¹⁶ are able to identify several other

of the 10 optical modes expected at small wave vectors,¹⁷ however, the results are not all unambiguous. In any case, it appears that no phonon frequencies will be larger than about 4.5 THz and therefore, all of the branches will be participating in thermal excitations even before room temperature is reached. The low frequencies are a result of the heavy atomic masses and the relatively weak bonding which gives rise to small interatomic force constants. The low melting point of 259°C is a further consequence of the overall low phonon frequencies and lattice softness. Force-constant parameters for phenomenological phonon models have been proposed,¹⁸ but they are not unique. We believe further neutron scattering experiments may be necessary to sort out the higher optical branches and to provide sufficient data for an unambiguous phonon model. From such a model the phonon eigenvectors for the modes at Γ could be obtained, and by then calculating the perturbation in the electronic structure caused by the atomic displacements for a particular phonon, the electron-phonon scattering matrix elements could be evaluated. For HgI_2 , the calculation is simplified to those phonons near Γ because of the direct gap, but such a calculation remains extremely difficult and has never been attempted.

In principle, measurement of the mobility at very low temperatures eliminates the dominance of the phonon scattering and provides some indication of the degree of impurity scattering. To our knowledge, the only measurements of mobilities made below 10 K on HgI_2 were reported by Bloch *et al.*¹⁹ They obtained large photocurrents and made Hall-effect and magnetoconductivity measurements. With excitation wavelengths greater than 5300 Å, they found only holes responsible for the conductivity (the electrons were assumed to be trapped at these temperatures), and were able to obtain hole mobilities parallel and perpendicular to the c axis for several samples. They report that the absolute value of the hole mobilities varied from sample to sample by up to an order of magnitude, but that the ratio of the in-plane to the c -axis mobility remained about 2.²⁰ Values of the hole mobility of up to 60 000 cm^2/Vs were measured at low temperatures. The larger in-plane hole mobility is consistent with our calculated smaller in-plane mass for the holes; however, the calculated c -axis to in-plane mass ratio is 0.22 and not 0.5. This difference in ratio could arise from anisotropy in the scattering from impurities. For example, impurities residing between the two iodine layers might be more effective in scattering carriers moving within the plane rather than along the c axis. Further measurements on well-characterized (perhaps purposely doped) samples as well as further calculations for impurity scattering could clearly be useful.

ACKNOWLEDGMENTS

This work was supported by EG&G Energy Measurements, Santa Barbara Operations, Goleta, CA. The authors are grateful to the staff at EG&G for useful conversations and for providing them with technical information relating to mercuric iodide. Correspondence with B. Prevot has also been helpful.

- ¹An extensive review of the physical properties of α -HgI₂ is contained in a report by M. Piechotka and E. Kaldis, Laboratorium, für Festkörperphysik, Eidgenössische Technische Hochschule-Zürich, Report No. CH-8093, Zürich, 1984 (unpublished).
- ²G. Ottaviani, C. Canali, and A. Alberigi Quaranta, IEEE, Trans. Nucl. Sci. NS-22, 192 (1975); R. Minder, G. Ottaviani, and C. Canali, J. Phys. Chem. Solids. 37, 417 (1976).
- ³L. van den Berg and W. F. Schnepfle, Nucl. Instrum. Methods B 44 (to be published).
- ⁴J. H. Yee, J. W. Sherohman, and G. A. Armantrout, IEEE Trans. Nucl. Sci. NS-23, 117 (1976).
- ⁵G. A. Jeffrey and N. Vlasse, Inorg. Chem. 6, 396 (1967).
- ⁶D. D. Koelling and B. N. Harmon, J. Phys. C 10, 3107 (1977).
- ⁷L. Hedin and B. I. Lundqvist, J. Phys. C 4, 2064 (1971).
- ⁸D. D. Koelling and G. O. Arbman, J. Phys. F 5, 2041 (1975).
- ⁹B. V. Novikov and N. N. Pimonenko, Fiz. Tekh. Poluprovodn. 4, 2077 (1970) [Sov. Phys.—Semicond. 4, 1785 (1971)].
- ¹⁰See W. Hanke and L. J. Sham, Phys. Rev. B 38, 13 361 (1988), and references therein.
- ¹¹J. Rath and A. J. Freeman, Phys. Rev. B 11, 2109 (1975).
- ¹²For a discussion of this so-called “ $\frac{2}{3}$ rds” rule for spin-orbit splitting in tetragonal crystals, see M. Cardona, *Modulation Spectroscopy* (Academic, New York, 1969); p. 69.
- ¹³S. Haussühl and H. Scholz, Krist. Tech. 10, 1175 (1975).
- ¹⁴Preliminary data by V. Garrish at EG&G Measurements, Santa Barbara, CA suggest a higher mobility for holes perpendicular to the *c* axis (private communication).
- ¹⁵B. Prevot, C. Schwab, and B. Dorner, Phys. Status, Solidi B 88, 327 (1978).
- ¹⁶S. Nakashima and M. Balkanski, Phys. Rev. B 34, 5801 (1986), and references therein.
- ¹⁷M. Sieskind, J. Phys. Chem. Solids 39, 1251 (1978).
- ¹⁸Models and force constants based on information of phonons at the Γ point have been given by N. Krauzman, M. Krauzman, and H. Poulet, C. R. Acad. Sci. (Paris) B 273, 301 (1971).
- ¹⁹P. D. Bloch, J. W. Hodby, T. E. Jenkins, D. W. Stacey, and C. Schwab, Nuovo Cimento 38B, 337 (1977).
- ²⁰P. D. Bloch, J. W. Hodby, C. Schwab, and D. W. Stacey, J. Phys. C 11, 2579 (1978).